Electronic Supplementary Information

Tailoring the energy band in flexible photodetectors based on transferred ITO/Si heterojunctions via interface engineering

*Guang Yao, Taisong Pan, Zhuocheng Yan, Feiyi Liao, Sihong Chen, Hulin Zhang, Min Gao and Yuan Lin**

State Key Laboratory of Electronic Thin Films and Integrated Devices, University of Electronic Science and Technology of China, Chengdu, Sichuan 610054, P. R. China

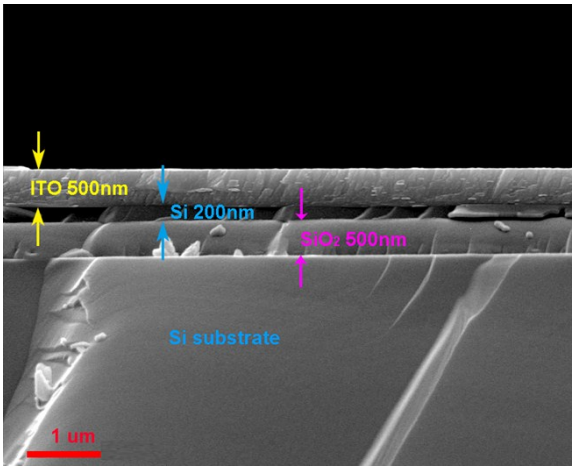

Figure S1. A typical cross-sectional SEM image of the ITO/SOI samples.

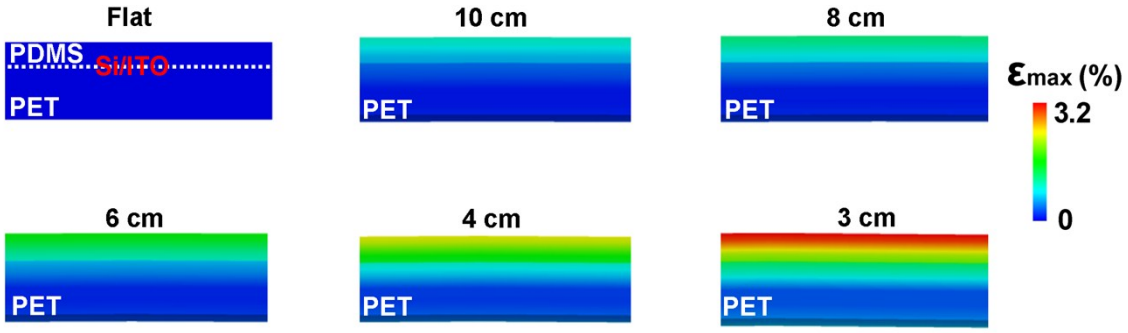

Figure S2. Simulation results of strains in the section-view of the small center area of the heterojunction being bent with different bending radii.

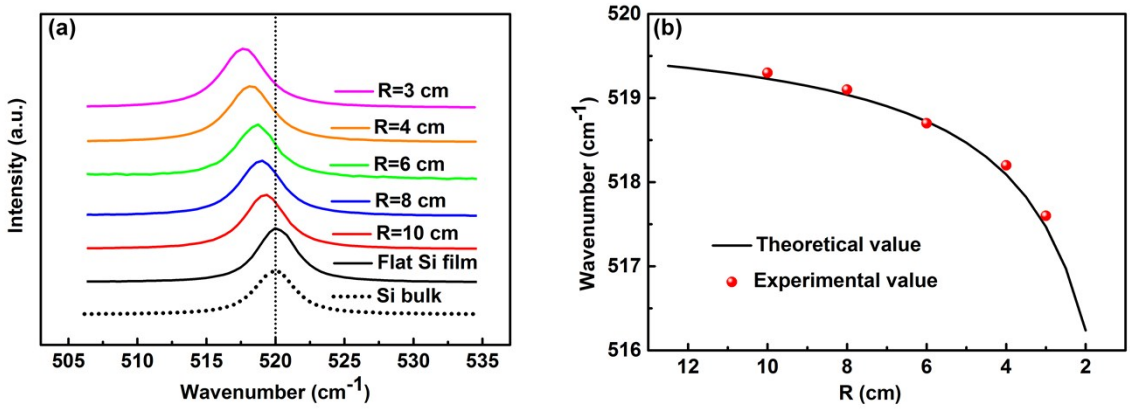

Figure S3. (a) Raman spectra of bulk Si and the transferred Si film being bent with different bending radii. (b) The theoretical and experimental Si Raman peaks for the transferred Si film bent with different bending radii.

Mechanical strain or stress may affect the frequencies of the Raman modes. The Raman spectra of bulk Si and the transferred Si film being bent with different bending radii were shown in Fig. S3 (a). It is found that with the decrease of bending radius, which means that the uniaxial stretching strain increases, the Raman peak shifts to the right.

For uniaxial stress σ along [100] direction, the Si Raman shift can be expressed as the following formula:[1]

$$\Delta\omega = \frac{1}{2\omega_0}[pS_{12} + q(S_{11} + S_{12})]\sigma \qquad (1)$$

where p ($p = -1.43\,\omega_0^2$) and q ($q = -1.89\,\omega_0^2$) are material constants, the so-called phonon deformation potentials, and S_{ij} ($S_{11} = 7.68\times10^{-2}$ Pa^{-1}, $S_{12} = -2.14\times10^{-12}$ Pa^{-1}) are the elastic compliance tensor elements of silicon. The formula above can be shown as:

$$\Delta\omega = -2\times10^{-9}\sigma = -180\varepsilon_{interface} = -180\times\frac{43um}{R+57.4um} \qquad (2)$$

As shown in Fig. S3 (b), the experimental results are well in line with the theoretical results, suggesting the model is reasonable to study the ITO/Si heterojunction under bending strains.

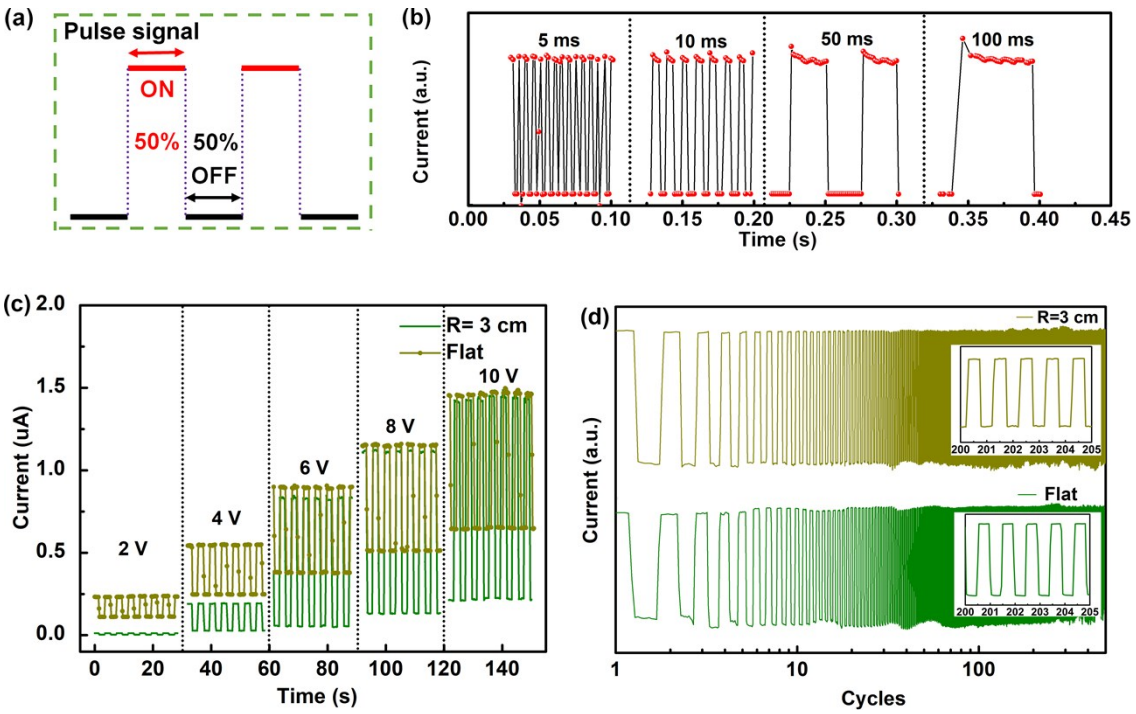

Figure S4. (a) Schematic diagram of the periodic on/off irradiation. (b) Response of the detector at the on/off radiation with different on–off periods. (c) Photocurrent at different bias for flat sample and bending sample with 3 cm bending radius. (d) Long-term stability of the samples at bias 5 V.

Photoresponsivity (R_λ), detectivity (D^*) and linear dynamic range (LDR) are important parameters of the photodetectors to evaluate the ability of converting the light signals and measure the detector sensitivity under a certain wavelength. R_λ can be defined as:

$$R_\lambda = I_{ph}/P_{Light} \quad (1)$$

where $I_{ph} = I_{Light} - I_{dark}$ is photocurrent and P_{Light} is illumination light power.

For the photodetectivity, there are three contributions to the noise that limit D^*:[3-5] shot noise from dark current, Johnson noise, and thermal fluctuation "flicker" noise. In our experiment, the shot noise from the dark current is the major contribution. The detectivity can be expressed as:

$$D^* = R_\lambda/(2qI_{dark})^{1/2} = (I_{ph}/P_{Light})/(2qI_{dark})^{1/2} \quad (2)$$

where q is the absolute value of electron charge (1.6×10^{-19} C) and I_{dark} is the dark current.

Another figure of merit for photodetectors is the linear dynamic range (LDR). LDR (typically quoted in dB) can be expressed as:[4, 5]

$$LDR = 20\log (I_{ph}/I_{dark}) \quad (3).$$

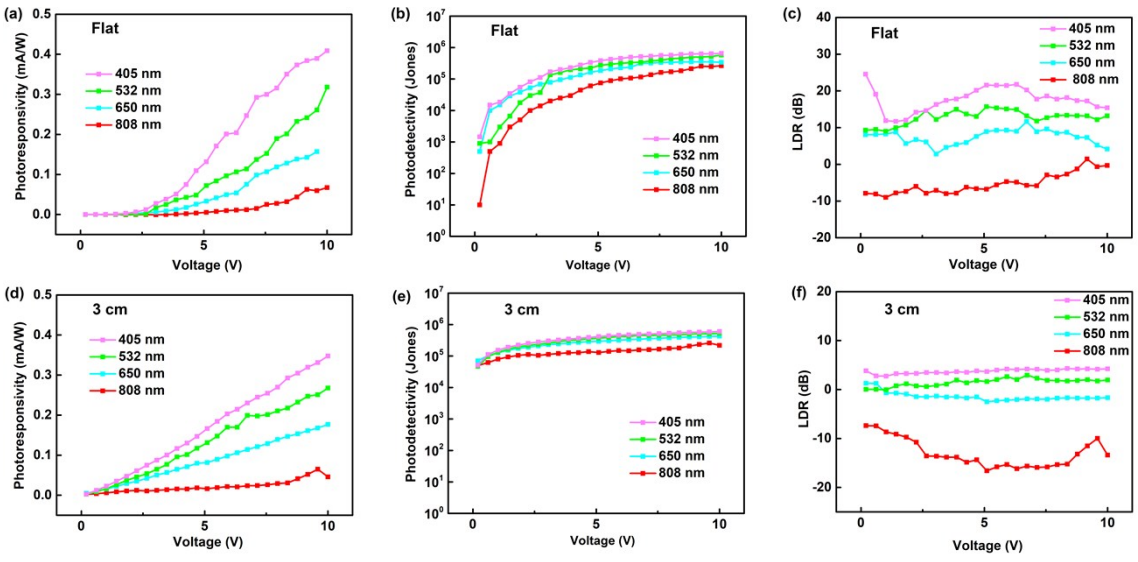

Figure S5. Photoresponsivity (Figures a and d), detectivity (Figures b and e) and linear dynamic range (Figures c and f) of the photodetector as a function of excitation wavelengths and bias for flat sample and sample with 3 cm bending radius.

By using the equations (1-3) shown above, R_λ, D^* and LDR at different wavelengths, corresponding to bending radius 0 cm and 3 cm, are shown in Figure S5. As shown in the Figures S5a and d, strong dependence of photoresponsivity on the light wavelength and bias can be observed in both cases. For semiconductor photodetectors, applying a bias voltage is an effective way to shorten the carriers' transit time by providing a stronger electric field to accelerate the photo-induced carriers reaching the electrodes, thus reducing the possibility of recombination. So the increase of bias leads to a higher photoresponsivity. In addition, it can be seen that for the flat photodetector (bending radius = 0 cm), the relation between bias and photoresponsivity is a non-linear one. The slope of the flat sample becomes larger with the increase of the bias, whereas that of the sample with 3 cm bending radius keeps almost the same. The difference of slope is the result of the transition of interface contact type from Schottky junction to Ohmic junction. Detectivity (Figures S5b and e) and linear dynamic range (Figures S5c and f) were also measured with irradiating light of different wavelengths. The results reflect that the bending strain also has significant influence on the detectivity and linear dynamic range of as-fabricated photodetector. Stable detectivity and linear dynamic range can be obtained when the photodetector was bent with bending radius 3 cm, which can be attributed to the Ohmic contact brought by the uniaxial mechanical bending strain.

References

1. I. D. Wolf, *Semicond. Sci. Tech.*, 1996, **11**, 139.
2. Y. Xie, B. Zhang, S. Wang, D. Wang, A. Wang, Z. Wang, H. Yu, H. Zhang, Y. Chen and M. Zhao, *Adv. Mater.*, 2017, **29**, 1605972.
3. S. R. Tamalampudi, Y. Y. Lu, U. R. Kumar, R. Sankar, C. D. Liao, B. K. Moorthy, C. H. Cheng, F. C. Chou and Y. T. Chen, *Nano Lett.*, 2014, **14**, 2800.
4. X. Gong, M. Tong, Y. Xia, W. Cai, J. S. Moon, Y. Cao, G. Yu, C. L. Shieh, B. Nilsson and A. J. Heeger, *Science*, 2009, **325**, 1665.
5. X. Li, M. Zhu, M. Du, Z. Lv, L. Zhang, Y. Li, Y. Yang, T. Yang, X. Li and K. Wang, *Small*, 2016, **12**, 595.